Viscosity of ice-in-oil slurries

Madina Naukanova, Gianluca Lavalle, Jean-Michel Herri, Ana Cameirao,
Pavel G. Struchalin, Boris V. Balakin

Viscosity of ice-in-oil slurries
Viscosité des coulis de glace à base d'huile

Madina Naukanova [a,*], Gianluca Lavalle [a], Jean-Michel Herri [a], Ana Cameirao [a],
Pavel G. Struchalin [b], Boris V. Balakin [b,*]

[a] *Mines Saint-Étienne, Univ Lyon, CNRS, UMR 5307 LGF, Centre SPIN, F - 42023 Saint-Étienne, France*
[b] *Western Norway University of Applied Sciences, Bergen, Norway*

ARTICLE INFO

ABSTRACT

Ice slurries are phase change materials extensively used in refrigeration technology. This work describes an experimental study and empirical modeling that was carried out to characterize the rheological behavior of ice-in-oil slurries. Decane and crushed ice were mixed to prepare test samples with ice volume percentages ranging from 3.5 to 17.7%. The size of the particles was 0.27 ± 0.13 mm. The viscosity measurements are performed at -2.5, -5.0, and $-10.0\,°C$ using a rotational viscometer with a three-bladed impeller. The maximum relative velocity was ~ 3.1 for 17.7% vol. concentration. A Bingham viscoplastic model was used to predict the rheological behavior of ice-in-oil slurries. The fractal dimension, packing limit, size of ice particles, and inter-particle cohesive forces were all considered in rheological calculations to make the model extensively applicable. The model accuracy is then examined using third-party experiments and experimental findings from the current study. The model appears to be a viable tool for predicting the viscosity of ice-in-oil slurries.

1. Introduction

Ice slurries are low-cost and environmentally friendly heat transfer fluids (O'Neill et al., 2021) containing the widely accessible phase change material (Esen, 2000; Esen and Ayhan, 1996). They are used in refrigeration technology (Kauffeld et al., 2005; Kauffeld and Gund, 2019). The slurries are applied both as coolants and thermal storage media. A conventional slurry contains particles of fresh-water ice dispersed in an aqueous solution. To preserve the ice particles yet to prevent the entire slurry from freezing, sodium chlorine or spirits are dissolved in water forming a base fluid (Monteiro and Bansal, 2010).

Ice slurries are multiphase systems with complex rheological behavior. There is a sufficient rheological database accumulated for slurries with an aqueous base. Bel (1996) measured the apparent viscosity of the slurry with 0.4 mm ice particles dispersed in an aqueous solution of ethanol at concentrations below 12%. Newtonian behavior of the slurry was detected. Lakhdar obtained similar results for an equivalent slurry with concentrations below 6%, while a pseudoplastic behavior was observed for concentrations up to 28%. Christensen and Kauffeld (1997) studied the slurry based on an ethanol solution with finer ice particles of 100 μm. They reported Newtonian behavior for concentrations below 15%. When the concentration was in the range 15...30%, the slurry turned into a Bingham fluid (Genovese et al., 2007a).

A massive database of rheological measurements was obtained for ice slurries indirectly by considering pressure loss imposed by ice particles in pipes. The studied systems were based on aqueous solutions of polypropylene (Stutz et al., 2000), propylene (Bellas et al., 2002), ethylene glycol (Lee et al., 2002), and brine (Illán and Viedma, 2009). In these works, the size of ice particles was in the range of 0.1...3.0 mm, and the ice concentration was below 30%. Monteiro and Bansal (2010) analyzed the indirect rheological data and found that most of the considered cases were described with the Herschel-Bulkley rheological model.

The aqueous base is less suitable for applications when a slurry goes through repeated cycles of melting and solidification (Matsumoto et al., 2000; Chibana et al., 2002). In this case, an original composition of the slurry might not reproduce in the cycles. To tackle this issue, melting ice particles may be dispersed in an oil base fluid, so they are able to turn into water and form an emulsion, which is further frozen again (Matsumoto et al., 2004, 2006). Slurries of ice in oil are also considered models for slurries of gas hydrates (Darbouret et al., 2005) and so applied in petroleum research (Yang et al., 2004). Although the ice particles in the oil-based slurry could be more cohesive than in an aqueous system (Aman et al., 2012) and so the rheology of the slurry should be sufficiently different, there was little published on that matter.

Matsumoto and Sonoda (2008), Matsumoto and Matsumoto (2009) measured the viscosity of ice slurry with an oil base formed by a lamp oil (Matsumoto and Sonoda, 2008) and medium chain triglycerides (Matsumoto and Matsumoto, 2009). The experiments were carried out at around −5.6 °C. The maximum size of the ice particles was in the range of 2.5...3.0 mm. The authors obtained similar results for both systems. The relative viscosity of the slurry was almost linearly dependent on the concentration of particles. The relative viscosity was about 3.0 at 20% of ice in the slurry; the maximum value was 4 at ~40%. The experimental results were not tested against the existing rheological models.

Lu and Sun (2021) produced an ice slurry freezing a water-paraffin emulsion. Prior to the solidification of ice particles, water was dispersed in nanosized droplets using a sonicator, and the emulsion was stabilized by sodium oleate and hexanol. The size of the ice particles further increased, and the maximum size became ~2 mm. The apparent viscosity of the slurry was studied in the temperature interval −3 to −1 °C. As follows from the rheological measurements, the relative viscosity was about 5.2 at ~40% wt., which is similar to Matsumoto's data considering the oil density difference (Matsumoto and Matsumoto, 2009). The maximum apparent viscosity was about 7 for ~58% wt., which is a notable solid loading for a homogeneous slurry. There was no rheological model proposed for the slurry.

Rensing et al. (2011) measured the viscosity of ice slurries formed from water-in-crude oil and brine-in-crude oil emulsions at −10.0 °C. The size of the droplets forming the particles was in the range 1.2...2.8 μm. The coalescence of the drops and the agglomeration of the frozen particles increased the particle size up to 1 mm. During the experiments, the slurry exhibited non-Newtonian behavior with a 20% vol. particle concentration, having a relative viscosity of 4 for the water-based ice and 7 for the brine-based ice. Yield stresses were 300...~3000 Pa for the concentrations in the interval 20%...60%. An increase in the particle concentration above 20% resulted in a dramatic increase of the relative viscosity to ~14 at 40% for the water-based slurry, while the viscosity reduced for the same concentration of the brine-based ice. The obtained rheological deviations are due to the difference in the surface energy and the cohesion of the considered types of ice particles. However, the Cross model used by the authors to approximate the results does not explicitly account for the observed phenomenon.

At the end of the literature overview, we conclude that there is no universal rheological model describing ice slurries with an oily base. The existing models are empirical and do not consider such an important phenomenon as cohesive interactions between the particles. Moreover, the granulometry of the ice is not taken into account by the so-far applied rheological expressions.

To address these uncertainties, we conduct rheological measurements in an ice slurry based on decane. Given the similarity between ice-in-oil slurries and gas hydrates, the proposed model can shed light on the rheological behavior of hydrates and help design hydrate management strategies. In the experiments, we accurately define both the concentration and size of the particles. Moreover, for the first time, we present an ice-in-oil slurry with known cohesion between the particles (Yang et al., 2004). The next aim of the study is to formulate a more realistic rheological model accounting for the sizes of the ice particles and their cohesion. We validate the model with our experiments and third-party data from the literature. Based on experimental findings, the potential of ice-decane slurry as a secondary refrigeration agent is examined.

2. Experiment

The viscosity of the slurry was measured using Bohlin Visco 88 viscometer. The viscometer was coupled with a 40 mm in-house impeller having three pitched blades. This impeller homogeneously dispersed the particles throughout the measurement. In the tests, a sample of
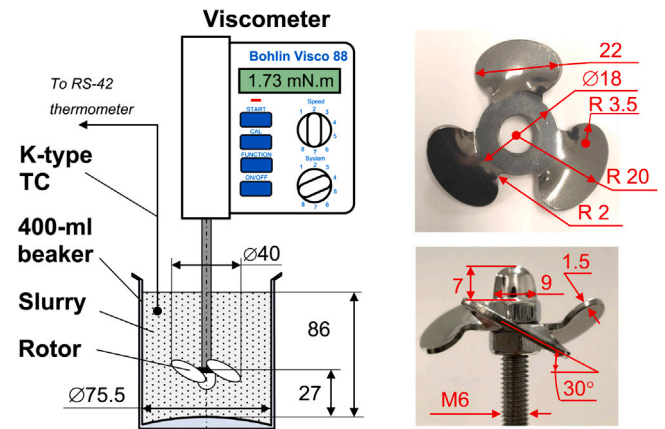

Fig. 1. Experimental setup.

liquid was placed in a 400 ml standard chemical beaker. The geometry of the experimental system and the impeller are shown in Fig. 1.

Using the non-standard impeller required calibration tests with single-phase fluids of known viscosity. We used pure decane, tap water, 35% vol. aqueous solutions of propylene glycol and ethylene glycol for the calibration tests. Table 1 displays the viscosity of the calibrating fluids and the corresponding torque values obtained from the viscometer. The calibration measurements were interpolated in Origin to obtain a correlation between the torque T on the viscometer's shaft and the measured viscosity μ: $\mu = 0.1306 \cdot \exp(3.8807 \cdot T)$.

For the measurement of the slurry viscosity, we used distilled water to manufacture ice cubes in a freezer at −22 °C. The ice was degassed using the procedure from the literature (Shamsutdinova et al., 2018). We used ice cubes mixed with a cold decane at −22 °C to produce the particles. The ice cubes filled with decane were milled in the BN750EU ice crusher from Ninja. The desirable volume concentration of ice was achieved by mixing the required masses of ice and decane. A fresh sample of the slurry was studied immediately after the production. The viscosity measurements were conducted at an ambient temperature of 22 ± 1 °C and atmospheric pressure. When the temperature of a fresh cold sample increased to −10 °C due to the heat transfer with the ambient, the measurements started. During the measurements, the torque at the impeller was recorded at a rotation speed of 572 rpm (No. in Visco 88). The viscosity was then computed from the torque using the calibration dataset. We measured the viscosity at different negative bulk temperatures during heating the sample from the ambient. The temperature of the slurry was controlled using a K-type thermocouple (±2.2 °C) connected to an RS PRO RS-42 datalogger (±0.1 °C). Rheological tests were conducted for a slurry with a 3.0 to 18.9% vol. particle concentration. Five series of measurements were carried out at three slurry temperatures for five selected particle concentrations within the specified range, resulting total of 75 measurements. Accurate reproducing of the slurry concentration from series to series was challenging, leading to variations around the selected value. Thus, based on the averaged data, all the measurements were summarized for the concentration range from 3.5 to 17.7% vol.

Experimental uncertainties

The uncertainty of the viscosity measurement is given as $\sigma = \sqrt{\sigma_s^2 + \sigma_i^2}$, where σ_s is the statistical error during measurements. The instrumental uncertainty σ_i is the error of the calibration correlation. It was defined as $\sigma_i = \sqrt{\sigma_r^2 + \sigma_d^2}$, where σ_r is the experimental uncertainty of the referent experiments (Huber et al., 2009; Anon, 2022; Huber et al., 2005; Hoga et al., 2018; Khattab et al., 2017). The latter uncertainty σ_d is the average deviation between the reference value from the literature and the viscosity of the calibrating liquid, which was re-calculated using the calibration correlation.

Table 1

The viscosity of calibrating fluids at $t = 21\,°C$ and $P = 0.1\,MPa$ retrieved from literature and torque values received from the viscometer at stirring rate $N = 572\,rpm$.

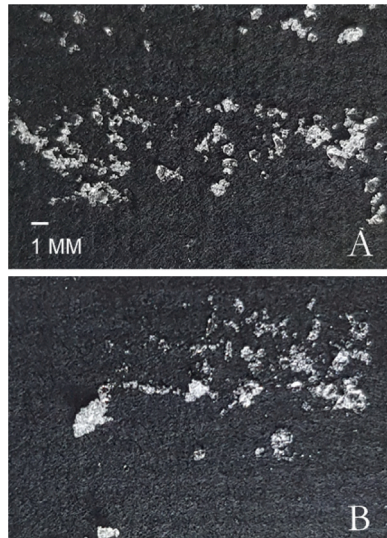| Fluids	Viscosity, [mPa s]	Torque [mN m]	Purity/Provider
Tap water	1.002 (Huber et al., 2009)	0.581	Bergen Vann (May 2022) (Anon, 2022)
Decane	0.903 (Huber et al., 2005)	0.448	>95 %/Avantor
Ethylene Glycol	19.735 (Hoga et al., 2018)	1.263	>99 %/Fybikon
Propylene Glycol (35% wt.)	2.880 (Khattab et al., 2017)	0.803	>95 %/Swed Handling

Fig. 2. Ice particles sampled from (A) fresh slurry and (B) after stirring by viscometer for 3 min at 60 rpm.
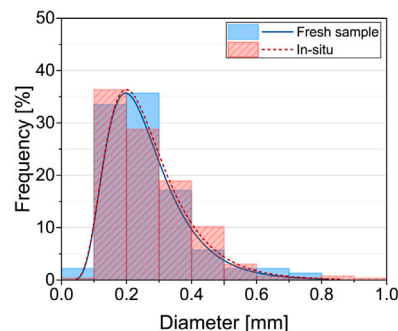

Fig. 3. Particle size distributions in fresh and in-situ samples.

3. Results and discussion

Particle size analysis

Like a majority of natural crystals, ice crystals vary in size. The diameter distribution of ice particles is among the factors controlling the inter-particle interaction. Fig. 2 contains pictures of ice particles collected from a freshly-made sample (Fig. 2A) and after stirring by the viscometer for 3 min (in-situ sample). The in-situ sample was agitated at the temperatures in the interval −22 °C to −2 °C (Fig. 2B).

After the preparation, both samples were placed in the freezer at −22 °C for 20 min for thermal stabilization. The ice particles in the image were distributed on 12 cm² flat plates with a scale. A black filter paper was placed beneath the particles to absorb residual decane and to achieve a good contrast. The particles were taken from the slurry with the aid of a straw. To prevent the melting of the particles, the equipment was placed inside the freezer well before the particles were studied. Again for thermal stabilization, the plate was put in the
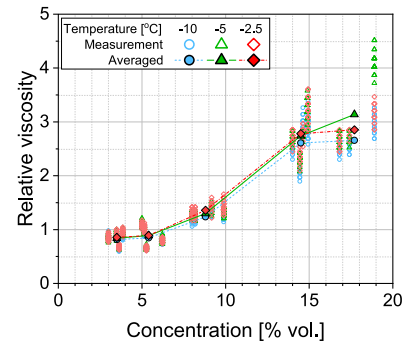

Fig. 4. Relative viscosity of ice-in-decane slurry at various temperatures and particle concentrations.

freezer for 10 min after spreading the particles. Then, pictures of the particles were taken with Leica Quad digital camera (20 MP, f/2.2, 16 mm). From Fig. 2, we note that the particles are transparent and non-uniform in shape and size. The pictures were treated using the ImageJ software, where the particles were detected and measured manually. Up to four pictures were treated for each sample. Fig. 3 summarizes the particle size distributions in the samples. The size of the particles varied from 0.09 to 0.96 mm. Particle size frequency is coherent with the log-normal curve. The average diameter of the particle was $0.27 \pm 0.13\,mm$ in both fresh and in-situ samples. This result is consistent with other works considering ice slurries (Stutz et al., 2000; Illán and Viedma, 2009). The average circularity was found to be 0.83 ± 0.03. As can be seen, the particle sizes for the samples are not significantly different from one another. This might be because the stirring time and rate were small enough to induce agglomeration.

Relative viscosity of the slurry

The relative viscosity of the slurry, calculated by Eq. (1), is shown in Fig. 4, and in Table 2 for various temperatures and particle concentrations. In Eq. (1), μ_a is the apparent viscosity of the slurry determined in the experiments, and μ_l is the viscosity of decane for a given temperature.

$$\mu_r = \frac{\mu_a}{\mu_l} \tag{1}$$

As can be seen, the relative viscosity of the slurry increases as the number of ice particles in the slurry increases. This is because a higher amount of particles provides stronger resistance on the impeller due to enhanced granular stresses in the slurry. The maximum relative viscosity of 3.1 was achieved at 17.7% vol., which is consistent with literature (Matsumoto et al., 2000). We also note that the relative viscosity increases with temperature at a given concentration. This is explained by the fact that the cohesion of ice grows with temperature (Yang et al., 2004). Relative viscosities of 3.5% vol. and 5.5% vol. slurries are below unity. Here an additional uncertainty arises due to a transition of flow regime. Indeed, following Lashgari et al. (2014), the transition to the grain-inertia regime happens at the ice concentration of about 5% vol.

Table 2
Relative viscosity of the ice-decane slurry at different temperatures and volume concentrations of ice.

Concentration % vol.	−10 °C	−5 °C	−2.5 °C
3.5	0.8	0.8	0.9
5.4	0.8	0.9	0.9
8.8	1.2	1.3	1.4
14.5	2.6	2.7	2.8
17.7	2.7	3.1	2.9

3.1. Rheological models

It is interesting to evaluate the correspondence of the existing rheological models to our experimental results. We consider the Bingham plastic fluid viscosity model (Genovese et al., 2007b):

$$\mu_m = \mu_a + \frac{\tau_y}{\gamma}, \tag{2}$$

where μ_a is the apparent viscosity of slurry, τ_y is yield stress, and γ is a shear rate. The apparent viscosity μ_a can be expressed using Thomas' equation (Balakin et al., 2018):

$$\mu_m = \mu_l \left[1 + 2.5\phi + 10.05\phi^2 + 0.00273e^{16.6\phi}\right] \tag{3}$$

where μ_l is the viscosity of the base fluid (decane), and ϕ is the volume concentration of solid particles.

The yield stress τ_y behavior is primarily governed by the volume of the particles, their size, and how they interact with one another. In this context, assessing the cohesive force between the ice particles is crucial. In line with Potanin et al. (1995), the yield stress can be expressed as:

$$\tau_y = \left(\frac{2}{5\pi}\right) \frac{F_c}{d_0^2} \left(\frac{\phi}{\phi_{max}}\right)^{\frac{3}{3-fr}} \tag{4}$$

where F_c is the cohesive force between ice particles, d_0 is the average diameter of particles, ϕ_{max} is the packing limit of dry particles, and fr is the fractal dimension. The fr is a dimensionless parameter, which describes the degree to which the shape of a solid particle deviates from the spherical (Genovese et al., 2007b). Struchalin et al. (2023) found that the ice particle fractal dimension is $fr = 2.57$. Following empirical correlations from Hoffmann and Finkers (1995), the packing limit of the ice particles was found as $\phi_{max} = 0.56$. However, we anticipate that the packing limit in the suspending medium may be lower than in a solid state. Thus, we took into account a variety of packing limits, including $\phi_{max} = 0.44$, 0.50, and 0.56. Finally, using linear interpolation of experimental data from the literature (Yang et al., 2004), the cohesive force F_c between ice particles at −2.5 °C was determined. Since all of the terms involved in the yield stress estimation have been presented, we can focus on obtaining the shear rate.

In the literature (Herri et al., 1999), the shear rate is defined as:

$$\dot{\gamma} = \sqrt{\frac{2}{15} \frac{\epsilon}{\nu_m}} \tag{5}$$

where ϵ is the turbulent energy dissipation rate and ν_m is slurry kinematic viscosity. To express the energy dissipation rate, we employed (Herri et al., 1999):
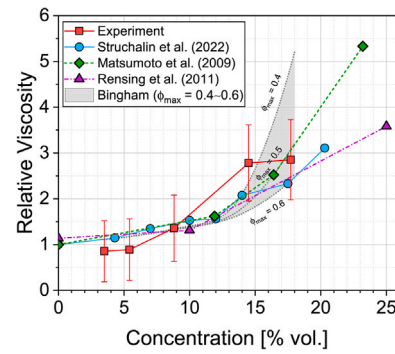
$$\epsilon = \frac{N_P N^3 D_S^5}{V} \tag{6}$$

where $V = 0.4 \cdot 10^{-3}$ m³ is the volume of analyzed slurry, $D_S = 0.04$ m is the diameter of the stirrer, N is the stirring rate, and N_P is the power number of the stirrer. The power number of the stirrer is a dimensionless number relating the resisting force to the inertial force:

$$N_P = \frac{P}{\rho_m N^3 D_S^5} \tag{7}$$

Substituting Eq. (7) into Eq. (6) gives:

$$\epsilon = \frac{P}{\rho_m V} \tag{8}$$

Fig. 5. Relative viscosity of ice-decane slurry at various particle concentrations. Experimental results at −2.5 °C (red squares, Table 2) are compared with experiments of Struchalin et al. (2023), Matsumoto and Matsumoto (2009), Rensing et al. (2011), and the rheological model (Eqs. (2)–(11)). (For interpretation of the references to color in this figure legend, the reader is referred to the web version of this article.)

where P is the power input implied on the viscometer and ρ_m is the density of the slurry. The power input is defined as a product of the angular velocity of the stirrer and torque T applied on the vertical shaft of the viscometer:

$$P = 2\pi N T \tag{9}$$

The density of the slurry ρ_m is given by:

$$\rho_m = \rho_l(1 - \phi) + \rho_s \phi \tag{10}$$

where ρ_s and ρ_l are the densities of ice and decane. And finally, the kinematic viscosity in Eq. (5) is given as (Mills, 1985):

$$\nu_m = \frac{\mu_a}{\rho_m} \tag{11}$$

Since all constituents of the model have been described, we can examine the model performance. The results of the rheological measurements are compared with the predictions of the models in Fig. 5, which is plotted with relative viscosity on the *y*-axis and slurry concentration on the *x*-axis. In addition, this figure provides the relative viscosity of ice-in-oil slurries considered in the literature (Struchalin et al., 2023; Rensing et al., 2011; Matsumoto and Matsumoto, 2009). The viscometer measurements of ice-decane slurry at −2.5 °C from the current investigation are displayed with associated uncertainties. Struchalin et al. (2023) produced ice-decane slurry viscosity values by correlating the pressure drop obtained during flow loop tests. We read from the figure that our results compare well to the dependence from Struchalin et al. (2023), and the deviations are due to the different particle sizes. The average and maximum deviation are 22.5% and 38.4%, respectively. Rensing et al. (2011) measured the viscosity of the ice slurry formed in an oil emulsion at −10 °C. Here, the average and the maximum deviations from our data are 23.8% and 39.0%. This difference may be due to the higher sphericity (and, therefore, circularity) of the particles in the study of Rensing et al. (2011). This potentially leads to lower viscosity of the particle suspensions (An et al., 2018). Matsumoto and Matsumoto (2009) measured the viscosity of the slurry formed from an emulsion. The deviations of our data from this dataset are 20.8% on average and 32.0% on maximum.

The unified model predictions (Eqs. (2)–(11)) are shown for different packing limits, including $\phi_{max} = 0.44$, 0.50, and 0.56. Less deviation from the experimental results can be observed with $\phi_{max} = 0.50$, which is 20.0% on average and 45.5% on maximum. It confirms that the packing limit of solid particles in the liquid phase is smaller than in the solid form.

4. Conclusions

In this study, we conducted rheological measurements for the ice slurry based on decane. We ran the experiments at negative temperatures down to $-10\,°C$ and particle concentration from 3.5 to 17.7% vol. The average diameter of the particles was 0.27 mm, and this value did not alter during the experiment. The measurement results indicate that the relative viscosity of the ice-decane slurry increases as both the particle concentration and temperature of the slurry increase. The maximum relative viscosity of ice-decane slurry is 3.1 at 17.7% vol. This moderate value means that the slurry is suitable for heat transfer applications. The obtained data have been compared with other studies of ice-in-oil slurry viscosity. As a result, the relative viscosity in our work has an average deviation of about 20% from the third-party data. The information regarding the rheological characteristics of ice-in-oil suspensions was expanded by our measurements. Bingham viscoplastic model was used to predict the viscosity of ice slurry. Unlike many empirical models, the current model considers particle size and inter-particle cohesion. The model is validated against our measurements and third-party experiments, with an average deviation of 20.0%. The model can be applied to predict the viscosity of PCM ice-slurries when designing the thermal process and controlling the operating conditions. In addition, given the similarity of ice-in-oil systems with hydrate slurries, this model is a valuable tool in the development of hydrate management strategies for flow assurance.

Declaration of competing interest

The authors declare the following financial interests/personal relationships which may be considered as potential competing interests: Boris V. Balakin reports financial support was provided by Research Council of Norway.

Acknowledgment

References

Aman, Z.M., Joshi, S.E., Sloan, E.D., Sum, A.K., Koh, C.A., 2012. Micromechanical cohesion force measurements to determine cyclopentane hydrate interfacial properties. J. Colloid Interface Sci. 376 (1), 283–288. http://dx.doi.org/10.1016/j.jcis.2012.03.019.

An, Z., Zhang, Y., Li, Q., Wang, H., Guo, Z., Zhu, J., 2018. Effect of particle shape on the apparent viscosity of liquid–solid suspensions. Powder Technol. 328, 199–206. http://dx.doi.org/10.1016/j.powtec.2017.12.019.

Anon, 2022. Tap water composition. https://www.bergen.kommune.no/innbyggerhjelpen/vann-vei-og-trafikk/vann-og-avlop/vann-og-vannforsyning/drikkevannskvalitet. (Accessed 21 October 2022).

Balakin, B.V., Kosinska, A., Kutsenko, K.V., 2018. Pressure drop in hydrate slurries: Rheology, granulometry and high water cut. Chem. Eng. Sci. 190, 77–85. http://dx.doi.org/10.1016/j.ces.2018.06.021.

Bel, O., 1996. Contribution à l'étude du comportement thermo-hydraulique d'un mélange diphasique dans une boucle frigorifique à stockage d'énergie (Ph.D. thesis). Lyon, INSA.

Bellas, J., Chaer, I., Tassou, S., 2002. Heat transfer and pressure drop of ice slurries in plate heat exchangers. Appl. Therm. Eng. 22 (7), 721–732. http://dx.doi.org/10.1016/S1359-4311(01)00126-0.

Chibana, K., Kang, C., Okada, M., Matsumoto, K., Kawagoe, T., 2002. Continuous formation of slurry ice by cooling water–oil emulsion in a tube. Int. J. Refrig. 25 (2), 259–266. http://dx.doi.org/10.1016/S0140-7007(01)00087-1.

Christensen, K., Kauffeld, M., 1997. Heat transfer measurements with ice slurry. In: IIR/IIF International Conference on Heat Transfer Issues on Natural Refrigerants.

Darbouret, M., Cournil, M., Herri, J.-M., 2005. Rheological study of TBAB hydrate slurries as secondary two-phase refrigerants. Int. J. Refrig. 28 (5), 663–671. http://dx.doi.org/10.1016/j.ijrefrig.2005.01.002.

Esen, M., 2000. Thermal performance of a solar-aided latent heat store used for space heating by heat pump. Sol. Energy 69 (1), 15–25. http://dx.doi.org/10.1016/S0038-092X(00)00015-3.

Esen, M., Ayhan, T., 1996. Development of a model compatible with solar assisted cylindrical energy storage tank and variation of stored energy with time for different phase change materials. Energy Convers. Manage. 37 (12), 1775–1785. http://dx.doi.org/10.1016/0196-8904(96)00035-0.

Genovese, D.B., Lozano, J.E., Rao, M., 2007a. The rheology of colloidal and noncolloidal food dispersions. J. Food Sci. 72 (2), R11–R20. http://dx.doi.org/10.1111/j.1750-3841.2006.00253.x.

Genovese, D.B., Lozano, J.E., Rao, M.A., 2007b. The rheology of colloidal and noncolloidal food dispersions. J. Food Sci. 72, http://dx.doi.org/10.1111/J.1750-3841.2006.00253.X.

Herri, J.-M., Pic, J.-S., Gruy, F., Cournil, M., 1999. Methane hydrate crystallization mechanism from in-situ particle sizing. AIChE J. 45 (3), 590–602. http://dx.doi.org/10.1002/aic.690450316.

Hoffmann, A., Finkers, H., 1995. A relation for the void fraction of randomly packed particle beds. Powder Technol. 82 (2), 197–203. http://dx.doi.org/10.1016/0032-5910(94)02910-G.

Hoga, H.E., Torres, R.B., Volpe, P.L.O., 2018. Thermodynamics properties of binary mixtures of aqueous solutions of glycols at several temperatures and atmospheric pressure. J. Chem. Thermodyn. 122, 38–64. http://dx.doi.org/10.1016/j.jct.2018.02.022.

Huber, M.L., Laesecke, A., Xiang, H.W., 2005. Viscosity correlations for minor constituent fluids in natural gas: n-octane, n-nonane and n-decane. Fluid Phase Equilib. 228–229, 401–408. http://dx.doi.org/10.1016/j.fluid.2005.03.008, PPEPPD 2004 Proceedings.

Huber, M.L., Perkins, R.A., Laesecke, A., Friend, D.G., Sengers, J.V., Assael, M.J., Metaxa, I.N., Vogel, E., Mareš, R., Miyagawa, K., 2009. New international formulation for the viscosity of H2O. J. Phys. Chem. Ref. Data 38 (2), 101–125. http://dx.doi.org/10.1063/1.3088050.

Illán, F., Viedma, A., 2009. Prediction of ice slurry performance in a corrugated tube heat exchanger. Int. J. Refrig. 32 (6), 1302–1309. http://dx.doi.org/10.1016/j.ijrefrig.2009.01.027.

Kauffeld, M., Gund, S., 2019. Ice slurry–History, current technologies and future developments. Int. J. Refrig. 99, 264–271. http://dx.doi.org/10.1016/j.ijrefrig.2019.01.010.

Kauffeld, M., Kawaji, M., Egolf, P.W., 2005. Handbook on Ice Slurries, Vol. 359. International Institute of Refrigeration, Paris.

Khattab, I.S., Bandarkar, F., Khoubnasabjafari, M., Jouyban, A., 2017. Original article. Arab. J. Chem. 10 (S1), S71–S75. http://dx.doi.org/10.1016/j.arabjc.2012.07.012.

Lashgari, I., Picano, F., Breugem, W.-P., Brandt, L., 2014. Laminar, turbulent, and inertial shear-thickening regimes in channel flow of neutrally buoyant particle suspensions. Phys. Rev. Lett. 113 (25), 254502. http://dx.doi.org/10.1103/PhysRevLett.113.254502.

Lee, D., Yoon, C., Yoon, E., Joo, M., 2002. Experimental study on flow and pressure drop of ice slurry for various pipes. In: Proceedings of the 5th Workshop on Ice-Slurries of the International Institute of Refrigeration.

Lu, L., Sun, Z., 2021. Ice slurry formation and ice crystal growth by using paraffin microemulsion. Int. J. Refrig. 130, 434–440. http://dx.doi.org/10.1016/j.ijrefrig.2021.06.027.

Matsumoto, K., Matsumoto, K., 2009. Development of W/O emulsion to form harmless ice slurry to human being. Int. J. Refrig. 32 (3), 411–420. http://dx.doi.org/10.1016/j.ijrefrig.2008.09.005.

Matsumoto, K., Namiki, Y., Okada, M., Kawagoe, T., Nakagawa, S., Kang, C., 2004. Continuous ice slurry formation using a functional fluid for ice storage. Int. J. Refrig. 27 (1), 73–81. http://dx.doi.org/10.1016/S0140-7007(03)00102-6.

Matsumoto, K., Oikawa, K., Okada, M., Teraoka, Y., Kawagoe, T., 2006. Study on high performance ice slurry formed by cooling emulsion in ice storage (discussion on adaptability of emulsion to thermal storage material). Int. J. Refrig. 29 (6), 1010–1019. http://dx.doi.org/10.1016/j.ijrefrig.2005.12.013.

Matsumoto, K., Okada, M., Kawagoe, T., Kang, C., 2000. Ice storage system with water–oil mixture: formation of suspension with high IPF. Int. J. Refrig. 23 (5), 336–344. http://dx.doi.org/10.1016/S0140-7007(99)00073-0.

Matsumoto, K., Sonoda, S., 2008. Continuous ice slurry formation by using W/O emulsion with higher water content. Int. J. Refrig. 31 (5), 874–882. http://dx.doi.org/10.1016/j.ijrefrig.2007.10.003.

Mills, P., 1985. Non-Newtonian behaviour of flocculated suspensions. J. Physique Lett. 46, 301–309. http://dx.doi.org/10.1051/jphyslet:01985004607030100.

Monteiro, A.C., Bansal, P.K., 2010. Pressure drop characteristics and rheological modeling of ice slurry flow in pipes. Int. J. Refrig. 33 (8), 1523–1532. http://dx.doi.org/10.1016/j.ijrefrig.2010.09.009.

O'Neill, P., Fischer, L., Revellin, R., Bonjour, J., 2021. Phase change dispersions: A literature review on their thermo-rheological performance for cooling applications. Appl. Therm. Eng. 192, 116920. http://dx.doi.org/10.1016/j.applthermaleng.2021.116920.

Potanin, A.A., De Rooij, R., Ende, D.V.D., Mellema, J., 1995. Microrheological modeling of weakly aggregated dispersions. J. Chem. Phys. 102, 5845–5853. http://dx.doi.org/10.1063/1.469317.

Rensing, P.J., Liberatore, M.W., Sum, A.K., Koh, C.A., Sloan, E.D., 2011. Viscosity and yield stresses of ice slurries formed in water-in-oil emulsions. J. Non-Newton. Fluid Mech. 166 (14–15), 859–866. http://dx.doi.org/10.1016/j.jnnfm.2011.05.003.

Shamsutdinova, G., Hendriks, M.A., Jacobsen, S., 2018. Concrete-ice abrasion: wear, coefficient of friction and ice consumption. Wear 416, 27–35. http://dx.doi.org/10.1016/j.wear.2018.09.007.

Struchalin, P.G., Øye, V.H., Kosinski, P., Hoffmann, A.C., Balakin, B.V., 2023. Flow loop study of a cold and cohesive slurry. pressure drop and formation of plugs. Fuel 332, 126061. http://dx.doi.org/10.1016/j.fuel.2022.126061.

Stutz, B., Reghem, P., Martinez, O., 2000. Friction losses for flow of concentrated slurries. In: Proceedings of the Second Workshop on Ice Slurries of the IIR.

Yang, S.-o., Kleehammer, D.M., Huo, Z., Sloan, E.D., Miller, K.T., 2004. Temperature dependence of particle–particle adherence forces in ice and clathrate hydrates. J. Colloid Interface Sci. 277 (2), 335–341. http://dx.doi.org/10.1016/j.jcis.2004.04.049.